공학석사학위논문

Geometric Analysis and Optimization for FDI Performance of Redundant Inertial Sensors

중첩 관성센서의 고장검출 및 판별 성능에 대한 기하학적 분석 및 최적화

2016 년 8 월

서울대학교 대학원

기계항공공학부

김 현 진

Abstract

Geometric Analysis and Optimization for FDI Performance of Redundant Inertial Sensors

KIM, HYUN JIN
SCHOOL OF MECHNICAL AND
AEROSPACE ENGINEERING
COLLEGE OF ENGINEERING
SEOUL NATIONAL UNIVERSITY

This thesis suggests optimal configurations for redundant inertial sensors with analysis of geometric parameters with respect to Fault Detection and Identification (FDI). To define FDI performance of each configuration, a performance index for FDI method based on Parity Space Approach (PSA) is applied. Even though this index is dependent on the geometry of sensor configurations, however, it is hard to analyze the

performance index directly since it is expressed in the null space of Direction Cosine Matrix (DCM) for the configurations. To solve this limitation, a modified form of the FDI performance index is presented as a function of geometric parameter of the configurations. It makes the FDI performance analysis and optimization of the configurations much easier. Additionally, the optimizations of configurations such as platonic solids, single cones and dual cones are conducted by the modified performance index. Finally, the FDI performance of each configuration is compared with others by the FDI performance index. The comparison result shows that the optimized dual conic configurations achieve FDI performance superior to the one of other configurations. The same results are also confirmed by simulations and experiments on each configuration.

Keywords: Fault Detection and Identification (FDI), Redundant inertial sensor, Parity Space Approach, Performance index, Sensor Configuration, Optimization

Student Number: 2013-20666

Contents

List of Figures

List of Tables

Chapter 1

Introduction

1.1 Motivation and Background

Inertial sensors are fundamental components of Inertial Navigation System (INS) utilizes acceleration and angular rate measurements to calculate position and attitude of a body without external aids. For past decades, performance of the inertial sensor has been improved while its price has been decreased dramatically as MEMS technology has been developed. Now the inertial sensor is an essential component for modern navigation system from military, space applications [1,2] to even personal devices such as smartphone and amateur drones [3,4,5]. If unexpected faults occur on the sensors, however, it results in serious problems of navigation solutions since the solutions are achieved by integrating the measurements of inertial sensors. As the error of fault is integrated, the navigation solution may diverge [6]. Because of this reason, the inertial sensor requires high reliability and there are some Fault Detection and Identification (FDI) algorithms for the inertial sensors to mitigate the fault on the sensor measurements [7,8,9]. In general, the FDI algorithms for the systems require redundancies which mean surplus, duplicative function of another components of the systems. The redundancy of the system can be additional sensors or system

information from the mathematical models. Hwang et al. [7] defined the concept of the redundancy as illustrated in figure 1.1. In the concept of hardware redundancy, duplicative signals from various sensors are compared each other and the algorithms such as wavelet transformation and residual generation using Parity Space Approach (PSA) can be applied. On the other hand, states or values estimated by the algorithms such as Kalman filter using mathematical information are utilized for the residual generation in the concept of analytical redundancy. Though the analytical redundancy is more effective with respect to the system costs, hardware redundancy is more intuitive and easy to apply since it does not need to ensure the system robustness under the disturbances, uncertainties and noises [7]. Moreover, the redundant sets of hardware can be utilized to recover the system from the fault. In this reason, many systems considering high reliability basically adapt the hardware redundancy even they also applies analytical redundancies.

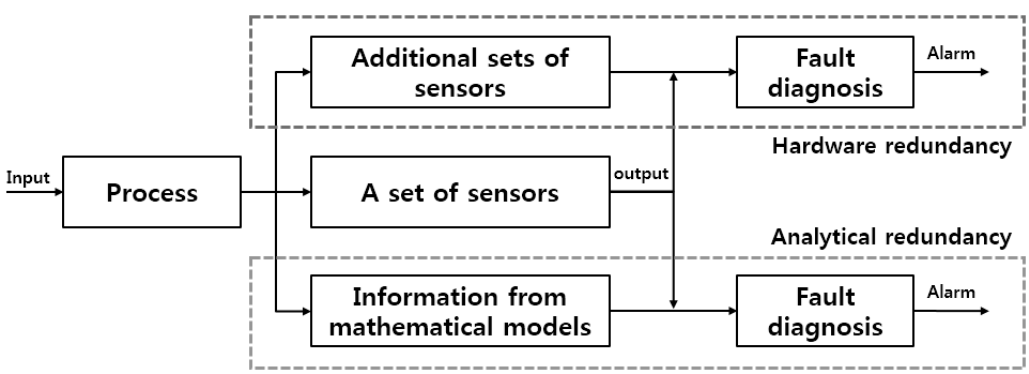

Figure 1.1 Concept of redundancy for FDI algorithm [7]

Meanwhile, Inertial Measurement Unit (IMU) in INS consists of at least three inertial sensors to estimate its states in three dimensional space. By using same types of sensors more than that, the IMU has hardware redundancy and is called Redundant IMU (RIMU) [6]. After Weiss and Nathan [10] firstly suggested the concept of RIMU, many researchers have been conducted studies on this topic. As practical examples of RIMU, Sukkarieh et al.[4] and Yoon et al.[5] applied RIMU to their drones. Moreover, a redundant gyro module is applied to the BILSAT-1, an earth observation satellite developed by cooperative research team of Surrey Satellite Technology (SSTL) and TÜBİTAK Space Technologies Research Institute [11]. Recently, Bittner et al. [12] introduced a cluster of IMU and Nilsson et al. [3] presented their open-source Multi IMU (MIMU) platform for pedestrian dead reckoning.

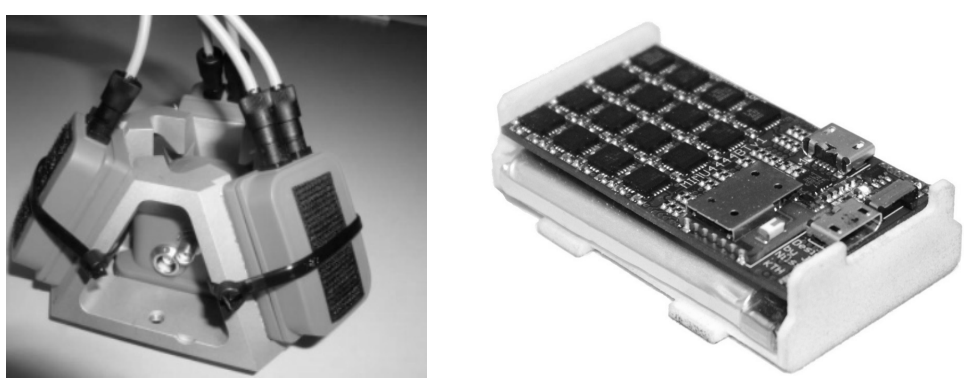

(a) Tetrahedron configuration [13] (b) RIMU on integrated circuit boards [14]

Figure 1.2 Examples of practical RIMU system

As theoretical approaches for RIMU, Wilcox [15] confirmed that PSA is appropriate for FDI of RIMU more than other methods. However, this result is acquired by numerical simulations and it is hard to compare various configurations with this method. To simplify this comparison process, Harrison and Gai [16] defined a performance index, also called Figure Of Merit (FOM), for PSA-based FDI. Since this index is dependent on the RIMU configuration, there exists optimal solution of sensor arrangement for FDI performance of RIMU. Therefore, various RIMU configurations are compared with each other in previous research [2,6,17,18,19,20] to find the optimal solution for FDI performance. However, there are few mathematical approaches to optimize the configurations with respect to the FDI of RIMU since it is hard to analyze the FDI performance index expressed in the null space of Direction Cosine Matrix (DCM) for RIMU configuration [16].

1.2 Objectives and Contributions

In the previous research with respect to the optimal configurations of RIMU, a lot of case studies and comparisons based on the performance index defined by Harrison [16] are conducted. However, Guidance, Navigation and Control (GNC) performance of RIMU has not been considered in the FDI performance comparisons and there has been no analytic approaches to find the optimal solutions in the previous research. The main objective of this thesis is to provide a base of the analytic approach for the

optimization of FDI performance index to overcome the limitations in previous research. In order that, a modified form of FDI performance index with respect to the angles between the inertial sensors is proposed to express the FDI performance of RIMU as a function of configuration geometry under the constraint for the optimal GNC performance. This modified index provides the base for the analysis of the FDI performance and make the optimization much easier and more reasonable. Another goal of this thesis is to validate the optimization using the proposed index. For this, the analytic optimization results are compared with numerical ones. Also, Monte Carlo simulations and experiments using 3D-printed frame are conducted to verify the comparison results of the index with the real FDI performance of RIMU.

1.3 Organization

This thesis is organized as follows. In chapter 2, sensor model and the performance index of RIMU defined in previous research are reviewed. Chapter 3 presents a modification of established FDI performance index. Using this modified FDI performance index, optimizations of the RIMU configurations are conducted and comparison results of the FDI performance index for each configurations are shown in chapter 4. To certify the result of the performance index optimization, simulations and experiments for real RIMU system are conducted in chapter 5. Finally, conclusions follow in section 6.

Chapter 2

Problem Formulation

2.1 Sensor Measurement Model

To define proper performance index for RIMU, mathematical model of inertial sensor measurements is required. The measurements of multiple inertial sensors on the RIMU are acquired as illustrated on figure 2.1 and they can be expressed in simple linear model as follows [16]:

$$\mathbf{m} = \mathbf{H}\mathbf{x} + \boldsymbol{\varepsilon},\ \mathbf{H} = \begin{pmatrix} \mathbf{h}_1 \\ \vdots \\ \mathbf{h}_n \end{pmatrix},\ \mathbf{x} = \begin{pmatrix} x_1 \\ x_2 \\ x_3 \end{pmatrix},\ \boldsymbol{\varepsilon} = \begin{pmatrix} \varepsilon_1 \\ \vdots \\ \varepsilon_n \end{pmatrix} \tag{2.1}$$

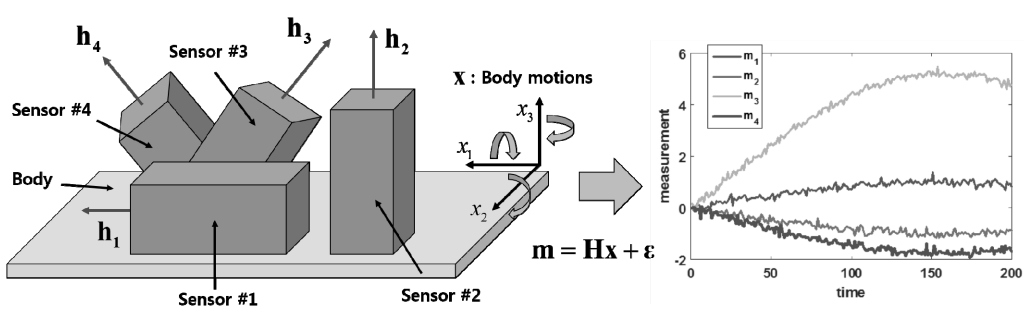

Figure 2.1 Measurement model of RIMU

where n is the number of sensors and $\mathbf{m} \in \mathbb{R}^n$ is a column vector of sensor measurements. DCM $\mathbf{H}$ consists of unit row vectors $\mathbf{h}_i$ aligned to the direction of i^{th} sensor. A column vector $\mathbf{x} \in \mathbb{R}^3$ represents states such as acceleration or angular rate of the body and $\boldsymbol{\varepsilon} \in \mathbb{R}^n$ is a column vector of Gaussian white noise whose property is as follows [16]:

$$\mathrm{E}(\boldsymbol{\varepsilon}) = \mathbf{0},\ \mathrm{E}(\boldsymbol{\varepsilon}\boldsymbol{\varepsilon}^{\mathbf{T}}) = \sigma^2 \mathbf{I}_n \tag{2.2}$$

where $\mathbf{I}_n$ is n^{th} identity matrix. It is assumed that all sensors have noise with the same standard deviation σ.

2.2 GNC Performance Index

Since the measurements of inertial sensors include stochastic noise, it is impossible to calculate exact value of state vector $\mathbf{x}$ with them. Therefore, proper estimation techniques such as least squares method are required. From the system model of (2.1), an estimated state vector $\hat{\mathbf{x}}$ is given as (2.3) by the least squares method [16].

$$\hat{\mathbf{x}} = (\mathbf{H}^{\mathrm{T}}\mathbf{H})^{-1}\mathbf{H}^{\mathrm{T}}\mathbf{m} \tag{2.3}$$

Because $\hat{\mathbf{x}}$ is not the exact solution, an estimation error $\mathbf{e}$ and its covariance $\mathbf{C}$ exist as follows [16]:

$$\mathbf{e} = \mathbf{x} - \hat{\mathbf{x}} \tag{2.4}$$

$$\mathbf{C} = \mathrm{E}(\mathbf{e}\mathbf{e}^{\mathrm{T}}) = \mathrm{E}\left[\left(\mathbf{x} - \hat{\mathbf{x}} \right) \left(\mathbf{x} - \hat{\mathbf{x}} \right)^{\mathrm{T}} \right] = \sigma^2 (\mathbf{H}^{\mathrm{T}}\mathbf{H})^{-1} \tag{2.5}$$

The smaller the estimation error is, the better navigation solution can be acquired. Therefore, the GNC performance of RIMU is related to the error covariance and the index for the GNC performance can be defined as (2.6) by normalizing the standard deviation σ [16].

$$\mathrm{FOM}_{\mathrm{GNC}} = \mathrm{trace}(\mathbf{C}) = \mathrm{trace}\left[(\mathbf{H}^{\mathrm{T}}\mathbf{H})^{-1} \right] \tag{2.6}$$

From the definition of (2.6), $\mathrm{FOM}_{\mathrm{GNC}}$ has to be minimized to optimize the navigation performance of RIMU since it is proportional to the estimation errors. Meanwhile, $\mathrm{FOM}_{\mathrm{GNC}}$ can be rewritten with the eigenvalues λ_1, λ_2 and λ_3 of $\mathbf{H}^{\mathrm{T}}\mathbf{H}$ and following Cauchy-Shwarz inequality is established [2] :

$$\mathrm{FOM}_{\mathrm{GNC}} = \mathrm{trace}(\mathbf{C}) = \lambda_1^{-1} + \lambda_2^{-1} + \lambda_3^{-1} \geq 3 \Big/ \sqrt[3]{\lambda_1 \lambda_2 \lambda_3} \tag{2.7}$$

Therefore, the optimal solution of $\mathrm{FOM}_{\mathrm{GNC}}$ is achieved when $\mathrm{FOM}_{\mathrm{GNC}}$ is minimized as the equality holds on. The constraint to hold on the equality in (2.7) is (2.8) and it results in (2.9) [2].

$$\lambda_1 = \lambda_2 = \lambda_3, \quad \mathrm{trace}\left[(\mathbf{H}^{\mathrm{T}}\mathbf{H})\right] = \lambda_1 + \lambda_2 + \lambda_3 = \mathrm{n} \tag{2.8}$$

$$\mathbf{H}^{\mathrm{T}}\mathbf{H} = \frac{\mathrm{n}}{3}\mathbf{I}_3 \tag{2.9}$$

Since the most important property of RIMU is a measurement accuracy, the condition for optimal GNC performance satisfying equation (2.9) is considered as a basic constraint in this thesis.

2.3 FDI Performance Index

Even though there are many methods for FDI of inertial sensors, PSA algorithm is one of the most famous methods to define the index for FDI performance. This method uses a parity vector $\mathbf{p}$ defined as follows [16]:

$$\mathbf{p} = \mathbf{V}\mathbf{m}, \quad \mathbf{p} = \begin{pmatrix} p_1 \\ \vdots \\ p_{\mathrm{n}} \end{pmatrix}, \mathbf{V} = \begin{pmatrix} \mathbf{v}_1 \\ \vdots \\ \mathbf{v}_{\mathrm{n}} \end{pmatrix} = \begin{pmatrix} v_{11} & \cdots & v_{1\mathrm{n}} \\ \vdots & \ddots & \vdots \\ v_{\mathrm{n}1} & \cdots & v_{\mathrm{nn}} \end{pmatrix} \tag{2.10}$$

where $\mathbf{v}_i^T$ is the null space of $\mathbf{H}^T$ so that $\mathbf{H}^T\mathbf{v}_i^T=\mathbf{0}$. It makes p_i independent to the state vector $\mathbf{x}$ which means that motion of the RIMU is excluded from FDI process. Additionally, p_i is a parity value to detect a fault on ith sensor. Therefore, it has to be insensitive to the fault on the sensors except ith one. It is satisfied when square sum of $\mathbf{v}_i$'s components except $v_{ii}=1$ is minimized as follows [16]:

$$\sum_{k=1,k\neq i}^{n} v_{ik}^2 \text{ is minimized to } v_{ii}=1 \tag{2.11}$$

To find the solution of $\mathbf{v}_i$ satisfying the condition (2.11), $\mathbf{v}_i^{(i)}$ and $\mathbf{H}^{(i)}$ are defined as $\mathbf{v}_i$ and $\mathbf{H}$ except their ith component v_{ii} and row vector $\mathbf{h}_i$ as follows:

$$\mathbf{v}_i^{(i)}=\begin{pmatrix} v_{i1} & \cdots & v_{i(i-1)} & v_{i(i+1)} & \cdots & v_{in} \end{pmatrix} \tag{2.12}$$

$$\mathbf{H}^{(i)}=\begin{pmatrix} \mathbf{h}_1^T & \cdots & \mathbf{h}_{i-1}^T & \mathbf{h}_{i+1}^T & \cdots & \mathbf{h}_n^T \end{pmatrix}^T \tag{2.13}$$

Then, $\mathbf{v}_i\mathbf{H}=\mathbf{0}_3$ can be rewritten as $\mathbf{v}_i^{(i)}\mathbf{H}^{(i)}+\mathbf{h}_i=\mathbf{0}$ and $\mathbf{v}_i^{(i)}$ is a solution of Lagrange equation following in (2.14) and (2.15) [6, 16].

$$\begin{pmatrix} 2\mathbf{I}_{(n-1)} & \mathbf{H}^{(i)} \\ \left(\mathbf{H}^{(i)}\right)^T & \mathbf{0} \end{pmatrix}\begin{pmatrix} \mathbf{v}_i^{(i)} \\ \eta \end{pmatrix}=\begin{pmatrix} \mathbf{0} \\ -\mathbf{h}_i \end{pmatrix} \tag{2.14}$$

$$\mathbf{v}_{\mathrm{i}}^{(\mathrm{i})} = -\mathbf{h}_{\mathrm{i}}\left[\left(\mathbf{H}^{(\mathrm{i})}\right)^{\mathrm{T}}\mathbf{H}^{(\mathrm{i})}\right]^{-1}\left(\mathbf{H}^{(\mathrm{i})}\right)^{\mathrm{T}} \tag{2.15}$$

where η is Lagrange multiplier. Meanwhile, the stochastic properties of p_{i} for each case of normal condition and fixed-bias fault on k[th] sensor are as follows [6, 16]:

$$\text{Normal condition: } \mathrm{E}(p_{\mathrm{i}}) = 0,\ \sigma_{p_{\mathrm{i}}}^2 = \mathbf{v}_{\mathrm{i}}\mathbf{v}_{\mathrm{i}}^{\mathrm{T}}\sigma^2 \tag{2.16}$$

$$\text{Fault on j-th sensor: } \mathrm{E}(p_{\mathrm{i}}) = v_{\mathrm{ij}}f_{\mathrm{j}},\ \sigma_{p_{\mathrm{i}}}^2 = \mathbf{v}_{\mathrm{i}}\mathbf{v}_{\mathrm{i}}^{\mathrm{T}}\sigma^2 \tag{2.17}$$

where σ is a standard deviation of sensor noise and f_{j} is a size of additive fault on j[th] sensor. Since sensitivity of p_{i} to the fault on j[th] sensor is related to ratio of $\mathrm{E}(p_{\mathrm{i}}) = v_{\mathrm{ij}}f_{\mathrm{j}}$ and $\sigma_{p_{\mathrm{i}}}^2 = \mathbf{v}_{\mathrm{i}}\mathbf{v}_{\mathrm{i}}^{\mathrm{T}}\sigma^2$, fault distance related to the sensitivity of p_{i} is defined as follows [6, 16]:

$$\mathrm{J}_{\mathrm{ij}} = \frac{v_{\mathrm{ij}}^2}{\mathbf{v}_{\mathrm{i}}\mathbf{v}_{\mathrm{i}}^{\mathrm{T}}} \tag{2.18}$$

It means the sensitivity of p_{i} to the fault on j[th] sensor. Also, it is hard to identify which sensor is in fault if J_{ii} is similar with J_{ij}. From this idea, the index for FDI performance of p_{i} is defined as follows [6, 16]:

$$\mathrm{FOM}_{p_i} = \frac{\mathrm{J_{ii}}}{\max_{\mathrm{j}} \mathrm{J_{ij}}(\mathrm{j} \neq \mathrm{i})} \tag{2.19}$$

If $\mathrm{FOM}_{p_i} = 1$, it means that the parity p_i for ith sensor cannot tell the fault on ith sensor and jth sensor since the fault distances for both cases are same. Additionally, $\mathrm{FOM_{FDI}}$ for whole sensors on RIMU is defined as (2.20) since RIMU including n-sensors has to consider the worst case of FOM_{p_i} [6, 16].

$$\mathrm{FOM_{FDI}} = \min_{\mathrm{i}} \left[\frac{\mathrm{J_{ii}}}{\max_{\mathrm{j}} \mathrm{J_{ij}}(\mathrm{j} \neq \mathrm{i})} \right] = \min_{\mathrm{i}} \left[\frac{1}{\max_{\mathrm{j}} v_{\mathrm{ij}}^2(\mathrm{j} \neq \mathrm{i})} \right] \tag{2.20}$$

2.4 Limitations of Previous Research

The aforementioned index for the GNC and FDI performance of RIMU is determined by the configurations of RIMU and it is remarkably helpful to compare the performance of each system without simulations or experiments for practical systems. However, the current form of the FDI performance index is not appropriate to express the FDI performance of RIMU as a function of geometric parameter directly related to the RIMU configuration since it is a function of null space components for the DCM of RIMU configuration. Therefore, it is hard to find the optimal configuration analytically

and that's why there have been only comparison results of case studies for some configurations in previous research. Moreover, the current form of the FDI performance index does not consider the constraint for the optimal solution of the GNC performance index. Therefore, a new form of FDI performance index considering geometric parameters of RIMU configuration and constraint for optimal GNC performance is required.

Chapter 3

Performance Index Modification

3.1 Geometric Parameter of Sensor Configuration

Limitations of the FDI performance index in previous research make hard to optimize the FDI performance of RIMU by configuration analysis. To solve this problem, a new vector $\mathbf{k}_i$ is defined as follows:

$$\mathbf{k}_i = \mathbf{H}\mathbf{h}_i^T = \begin{pmatrix} \cos\varphi_{i1} & \cdots & \cos\varphi_{in} \end{pmatrix}^T \tag{3.1}$$

where φ_{ij} is an included angle between the direction of $\mathbf{h}_i$ and $\mathbf{h}_j$ whose range is $0 \le \varphi_{ij} \le \pi$ in three-dimensional space. Then, $\mathbf{v}_i^{(i)}\mathbf{H}^{(i)} + \mathbf{h}_i = \mathbf{0}$ can be rewritten as (3.2) by multiplying $\mathbf{k}_i$ to the right side of its each term:

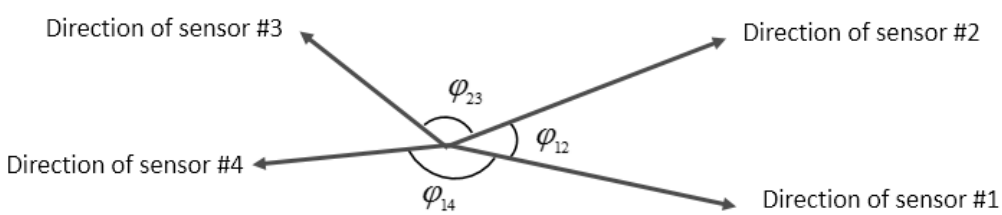

Figure 3.1 Illustration of direction cosine vectors and included angles

$$\mathbf{v}_i^{(i)}\mathbf{k}_i^{(i)} + 1 = 0 \tag{3.2}$$

where $\mathbf{k}_i^{(i)}$ is $\mathbf{k}_i$ except its i[th] components $\cos\varphi_{ii} = 1$. From the same logical flow of the FDI performance index definition in chapter 2 [16], $\mathbf{v}_i$'s components can be rewritten as follows:

$$\mathbf{v}_i^{(i)} = -\left[\left(\mathbf{k}_i^{(i)}\right)^T \mathbf{k}_i^{(i)}\right]^{-1}\left(\mathbf{k}_i^{(i)}\right)^T \tag{3.3}$$

$$v_{ii} = 1,\ v_{ij} = \frac{-\cos\varphi_{ij}}{\sum_{k=1,k\neq i}^{n}\cos\varphi_{ik}} (j \neq i) \tag{3.4}$$

It is only possible when there exists at least one sensor whose direction vector $\mathbf{h}_j (j \neq i)$ is not orthogonal to $\mathbf{h}_i$ so that $\mathbf{k}_i^{(i)} \neq \mathbf{0}$. If this condition is not satisfied, the output of i[th] sensor is independent to all other sensors. Then, FOM_{p_i} in (2.19) is not defined since $\mathbf{v}_i^{(i)}$ is singular as $\mathbf{H}^{(i)} = \mathbf{0}$ and there's no physical meaning for FDI of the RIMU. Therefore, it is assumed that this condition to derivate equation (3.3) from (3.2) is satisfied.

3.2 Modified Performance Index

By using the new parameter φ_{ij} in $\mathbf{k}_i$, the current FDI performance index can be expressed in a modified form considering the constraint for optimal GNC performance.

First, the optimal navigation constraint (2.9) can be rewritten as follows:

$$\mathbf{k}_i^{\mathrm{T}}\mathbf{k}_i = \left(\mathbf{H}\mathbf{h}_i^{\mathrm{T}}\right)^{\mathrm{T}}\left(\mathbf{H}\mathbf{h}_i^{\mathrm{T}}\right) = \frac{n}{3}\mathbf{h}_i\mathbf{h}_i^{\mathrm{T}} = \frac{n}{3} \tag{3.5}$$

$$\sum_{k=1,k\neq i}^{n}\cos\varphi_{ik} = \left(\mathbf{k}_i^{(i)}\right)^{\mathrm{T}}\mathbf{k}_i^{(i)} = \mathbf{k}_i^{\mathrm{T}}\mathbf{k}_i - 1 = \frac{n}{3} - 1 \tag{3.6}$$

It means that the denominator of v_{ij} in (3.4) is a constant for the number of sensors if the constraint for optimal GNC performance is satisfied. From this result, the modified FDI performance index proportional to the current one can be defined as follows:

$$\left(\mathrm{FOM}_{\mathrm{FDI}}\right)_{\mathrm{modified}} = \min_{i}\left[\frac{1}{\max\limits_{j\neq i}\cos^2\varphi_{ij}}\right] = \frac{1}{\varsigma\left(\varphi_{ij}\right)} \propto \mathrm{FOM}_{\mathrm{FDI}} \tag{3.7}$$

where $\varsigma\left(\varphi_{ij}\right) = \max\limits_{i,j}\left|\cos\varphi_{ij}\right|(j\neq i)$. Therefore, it is possible to optimize the FDI performance index by minimizing $\varsigma\left(\varphi_{ij}\right)$ since it is inversely proportional to the FDI performance index. In other words, the optimal solution for FDI performance of the RIMU can be determined by φ_{ij} of the RIMU configuration. Additionally, this result is based on the constraint of optimal GNC performance in (2.9). If this condition is not satisfied, the newly suggested form of the FDI performance index cannot be utilized and $\varsigma\left(\varphi_{ij}\right)$ is not acceptable for the optimization.

Chapter 4

Performance Index Optimization

4.1 Platonic Solid Configuration

A platonic solid is a geometric solid whose faces are all identical, regular polygons meeting at the same three-dimensional angles and there are only five solids as shown in figure 4.1 which meet this criteria. All of them satisfy the constraint for optimal GNC performance index if each sensor is placed along to the normal direction of each surface of the solids [2]. As one of the examples that meet the constraint for optimal GNC performance, sensor directions on the tetrahedron is shown in figure 4.2.

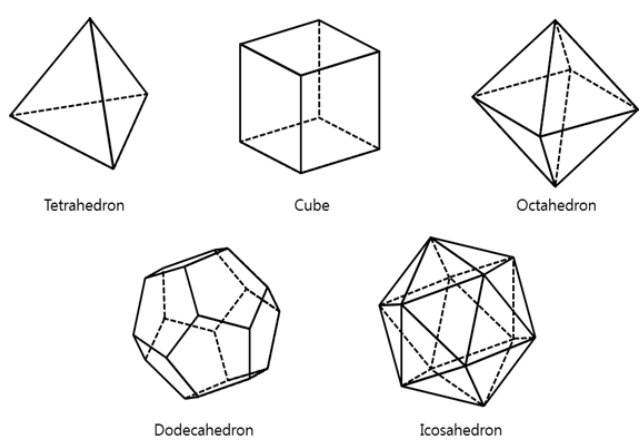

Figure 4.1 Platonic solids

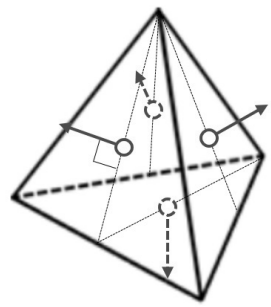

Figure 4.2 Optimal configuration for GNC performance : tetrahedron

In the same approach, DCM $\mathbf{H}$ of each platonic solid that satisfies the constraint for optimal GNC performance is shown in table 4.1.

Table 4.1 DCM $\mathbf{H}$ of platonic solids satisfying $\mathbf{H}^{\mathrm{T}}\mathbf{H} = \frac{\mathrm{n}}{3}\mathbf{I}_3$

Configuration	n	DCM $\mathbf{H}$
Tetrahedron (type 1)	4	$\mathbf{H}_{\mathrm{TET}} = \frac{1}{3}\begin{pmatrix} 2\sqrt{2} & 0 & 1 \\ -\sqrt{2} & \sqrt{6} & 1 \\ -\sqrt{2} & -\sqrt{6} & 1 \\ 0 & 0 & -3 \end{pmatrix}$
Cube (type 2)	6	$\mathbf{H}_{\mathrm{CUBE}} = \begin{pmatrix} 1 & 0 & 0 \\ 0 & 1 & 0 \\ 0 & 0 & 1 \\ -1 & 0 & 0 \\ 0 & -1 & 0 \\ 0 & 0 & -1 \end{pmatrix}$

Configuration	n	DCM **H**
Octahedron (type 3)	8	$\mathbf{H}_{\mathrm{OCT}} = \frac{1}{\sqrt{3}} \begin{pmatrix} \sqrt{2} & 0 & 1 \\ -\sqrt{2} & 0 & 1 \\ 0 & \sqrt{2} & 1 \\ 0 & -\sqrt{2} & 1 \\ \sqrt{2} & 0 & -1 \\ -\sqrt{2} & 0 & -1 \\ 0 & \sqrt{2} & -1 \\ 0 & -\sqrt{2} & -1 \end{pmatrix}$
Dodecahedron (type 4)	12	$\mathbf{H}_{\mathrm{DOD}} = \frac{1}{\sqrt{5}} \begin{pmatrix} 0 & 0 & \sqrt{5} \\ 0 & 0 & -\sqrt{5} \\ 2 & 0 & 1 \\ 2\cos(0.4\pi) & 2\sin(0.4\pi) & 1 \\ 2\cos(0.8\pi) & 2\sin(0.8\pi) & 1 \\ 2\cos(0.8\pi) & -2\sin(0.8\pi) & 1 \\ 2\cos(0.4\pi) & -2\sin(0.4\pi) & 1 \\ -2 & 0 & -1 \\ -2\cos(0.4\pi) & -2\sin(0.4\pi) & -1 \\ -2\cos(0.8\pi) & -2\sin(0.8\pi) & -1 \\ -2\cos(0.8\pi) & 2\sin(0.8\pi) & -1 \\ -2\cos(0.4\pi) & 2\sin(0.4\pi) & -1 \end{pmatrix}$

Configuration	n	DCM **H**
Icosahedron (type 5)	20	$\mathbf{H}_{\mathrm{ICO}} = \begin{pmatrix} \sin\alpha_1 & 0 & \cos\alpha_1 \\ \cos(0.4\pi)\sin\alpha_1 & \sin(0.4\pi)\sin\alpha_1 & \cos\alpha_1 \\ \cos(0.8\pi)\sin\alpha_1 & \sin(0.8\pi)\sin\alpha_1 & \cos\alpha_1 \\ \cos(0.8\pi)\sin\alpha_1 & -\sin(0.8\pi)\sin\alpha_1 & \cos\alpha_1 \\ \cos(0.4\pi)\sin\alpha_1 & -\sin(0.4\pi)\sin\alpha_1 & \cos\alpha_1 \\ \sin\alpha_2 & 0 & \cos\alpha_2 \\ \cos(0.4\pi)\sin\alpha_2 & \sin(0.4\pi)\sin\alpha_2 & \cos\alpha_2 \\ \cos(0.8\pi)\sin\alpha_2 & \sin(0.8\pi)\sin\alpha_2 & \cos\alpha_2 \\ \cos(0.8\pi)\sin\alpha_2 & -\sin(0.8\pi)\sin\alpha_2 & \cos\alpha_2 \\ \cos(0.4\pi)\sin\alpha_2 & -\sin(0.4\pi)\sin\alpha_2 & \cos\alpha_2 \\ -\sin\alpha_2 & 0 & -\cos\alpha_2 \\ -\cos(0.4\pi)\sin\alpha_2 & -\sin(0.4\pi)\sin\alpha_2 & -\cos\alpha_2 \\ -\cos(0.8\pi)\sin\alpha_2 & -\sin(0.8\pi)\sin\alpha_2 & -\cos\alpha_2 \\ -\cos(0.8\pi)\sin\alpha_2 & \sin(0.8\pi)\sin\alpha_2 & -\cos\alpha_2 \\ -\cos(0.4\pi)\sin\alpha_2 & \sin(0.4\pi)\sin\alpha_2 & -\cos\alpha_2 \\ -\sin\alpha_1 & 0 & -\cos\alpha_1 \\ -\cos(0.4\pi)\sin\alpha_1 & -\sin(0.4\pi)\sin\alpha_1 & -\cos\alpha_1 \\ -\cos(0.8\pi)\sin\alpha_1 & -\sin(0.4\pi)\sin\alpha_1 & -\cos\alpha_1 \\ -\cos(0.8\pi)\sin\alpha_1 & \sin(0.4\pi)\sin\alpha_1 & -\cos\alpha_1 \\ -\cos(0.4\pi)\sin\alpha_1 & \sin(0.4\pi)\sin\alpha_1 & -\cos\alpha_1 \end{pmatrix}$ $\cos\alpha_1 = \dfrac{1}{\sqrt{3}\tan\dfrac{\pi}{5}}$ $\cos\alpha_2 = \dfrac{1-\cos\dfrac{\pi}{5}}{\sqrt{3}\sin\dfrac{\pi}{5}}$

For the configurations on table 4.1, only case studies are possible since the configurations are fixed by the constraint of optimal GNC performance and there is no geometric parameter to adjust. The FDI performance index of platonic solid configurations in table 4.1 is shown in table 4.2.

Table 4.2 FDI performance index of platonic solids satisfying $\mathbf{H}^{\mathrm{T}}\mathbf{H} = \frac{\mathrm{n}}{3}\mathbf{I}_3$

Configurations	Tetrahedron (type 1)	Cube (type 2)	Octahedron (type 3)	Dodecahedron (type 4)	icosahedron (type 5)
$\mathbf{H}^{\mathrm{T}}\mathbf{H}$	$\frac{4}{3}\mathbf{I}_3$	$\frac{6}{3}\mathbf{I}_3$	$\frac{8}{3}\mathbf{I}_3$	$\frac{12}{3}\mathbf{I}_3$	$\frac{20}{3}\mathbf{I}_3$
$\mathrm{FOM}_{\mathrm{FDI}}$	1.0000	1.0000	2.7778	9.0000	32.1111

On table 4.2, it is confirmed that the RIMU using configuration type 1 and type 2 cannot identify which sensor is in fault since the FDI performance index is one [2] as mentioned in chapter 2.

4.2 Single Conic Configuration

A single conic configuration of RIMU is defined as the configuration that each sensor is evenly placed on the inclined plane of the cone and the origin of the direction cosine vectors of the sensors meet on the vertex of the cone as shown in figure 4.3. Unlike the platonic solid configurations, there are infinite conic configurations and there's no limit for the number of sensors to place.

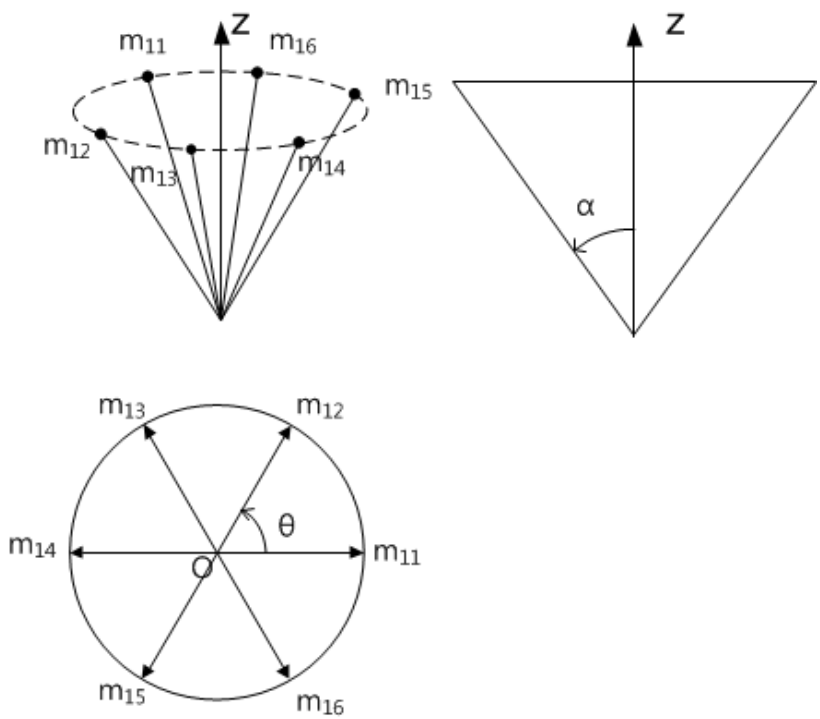

Figure 4.3 Single conic configuration

Normally, DCM $\mathbf{H}$ for the sensor orientations on single conic configuration is defined as follows:

$$\mathbf{H} = \begin{pmatrix} \mathbf{h}_1^T & \mathbf{h}_2^T & \cdots & \mathbf{h}_n^T \end{pmatrix}^T \tag{4.1}$$

$$\mathbf{h}_k = \begin{pmatrix} \cos\theta_k \sin\alpha & \sin\theta_k \sin\alpha & \cos\alpha \end{pmatrix} \tag{4.2}$$

where α is a center angle between inclined surface and z-axis of the cone while θ_k is an included angle between the sensors on the top view of configuration as shown in figure 4.3. The number k is an integer given along the counterclockwise direction in order of the nearest to the sensor set to $k=1$. In figure 4.3, for example, the number k is given as following orders; $k=2$ for m_{12}, $k=3$ for m_{13}, and $k=6$ for m_{16} if $k=1$ is set to m_{11}. Then, the included angle θ_k is as follows:

$$\theta_k = 2\pi(k\text{-}1)/n \quad (1 \le k \le n) \tag{4.3}$$

Therefore, the constraint of the optimal GNC performance in (2.9) is rewritten as follows by simple characteristics of the trigonometrical functions

$$\mathbf{H}^T\mathbf{H} = \sum_{k=1}^{n} \mathbf{h}_k^T \mathbf{h}_k = \frac{n}{3}\mathbf{I}_3 \tag{4.4}$$

$$\sum_{k=1}^{n}\mathbf{h}_k^T\mathbf{h}_k=\begin{pmatrix}\frac{n}{2}\sin^2\alpha & 0 & 0\\ 0 & \frac{n}{2}\sin^2\alpha & 0\\ 0 & 0 & n\cos^2\alpha\end{pmatrix} \tag{4.5}$$

Therefore, the α is fixed as $\alpha=\cos^{-1}\left(\sqrt{1/3}\right)=54.7356^\circ$. It means that there is no room for FDI performance optimization under the constraint for optimal GNC performance as well as the platonic solid configurations. Nevertheless, it is possible to assume some special cases which don't require the optimized GNC performance. Then, $\mathbf{v}_i^{(i)}$ for single conic configuration is determined as follows:

$$\mathbf{v}_i^{(i)}=-\mathbf{h}_i\left[\left(\mathbf{H}^{(i)}\right)^T\mathbf{H}^{(i)}\right]^{-1}\left(\mathbf{H}^{(i)}\right)^T=-\mathbf{h}_i\mathbf{A}^{-1}\left(\mathbf{H}^{(i)}\right)^T \tag{4.6}$$

$$\mathbf{A}^{-1}=\frac{4}{n^2(n-3)\sin^4\alpha\cos^2\alpha}\begin{pmatrix}a_{11} & 0 & a_{13}\\ 0 & a_{22} & 0\\ a_{13} & 0 & a_{33}\end{pmatrix} \tag{4.7}$$

$$a_{11}=\frac{n}{2}(n-1)\sin^2\alpha\cos^2\alpha \tag{4.8}$$

$$a_{22}=\frac{n(n-3)}{2}\sin^2\alpha\cos^2\alpha \tag{4.9}$$

$$a_{33}=\frac{n}{2}\left(\frac{n}{2}-1\right)\sin^4\alpha \tag{4.10}$$

$$a_{13}=\frac{n}{2}\sin^3\alpha\cos\alpha \tag{4.11}$$

Since $\theta_1 = 0$ from the definition in (4.3), v_{1j} is determined as follows:

$$v_{1j} = -\mathbf{h}_1 \mathbf{A}^{-1} \mathbf{h}_j^{\mathrm{T}} = \frac{1}{n-3}\left(1 + 2\cos\theta_j\right) \ (j \neq 1) \tag{4.12}$$

Therefore, the FDI performance index FOM_{p_1} for the first sensor axis is independent to the center angle α. Also, this result is same for any i=1, 2, ⋯, n since the single conic configuration is axial symmetric. Therefore, the FDI performance index of single conic configuration is determined as follows:

$$\mathrm{FOM}_{\mathrm{FDI}} = \left(\max_{j\,(j\neq 1)} \left[\frac{1}{(n-3)^2}\left(1 + 2\cos\theta_j\right)^2 \right] \right)^{-1} \tag{4.13}$$

This result of (4.13) means that the FDI performance index of the single conic configuration is determined by the number of sensors and independent to the center angle α. Therefore, the single conic configuration for RIMU cannot be optimized by geometric parameter α with respect to the FDI performance index when the number of sensors is fixed. From this reason, the optimal single conic configuration considering GNC and FDI performance is determined by the constraint of the optimal GNC performance in this thesis.

4.3 Dual Conic Configuration

The aforementioned configurations are very common for traditional RIMU. However, there is no room for geometric analysis of the FDI performance index for these configurations. Recently, Shim and Yang [2] suggested a concept of dual conic configuration as shown in figure 4.4 and compared its FDI performance index with the ones for other configurations by case studies. However, there is no analytic approach to optimize the FDI performance index of the dual conic configurations.

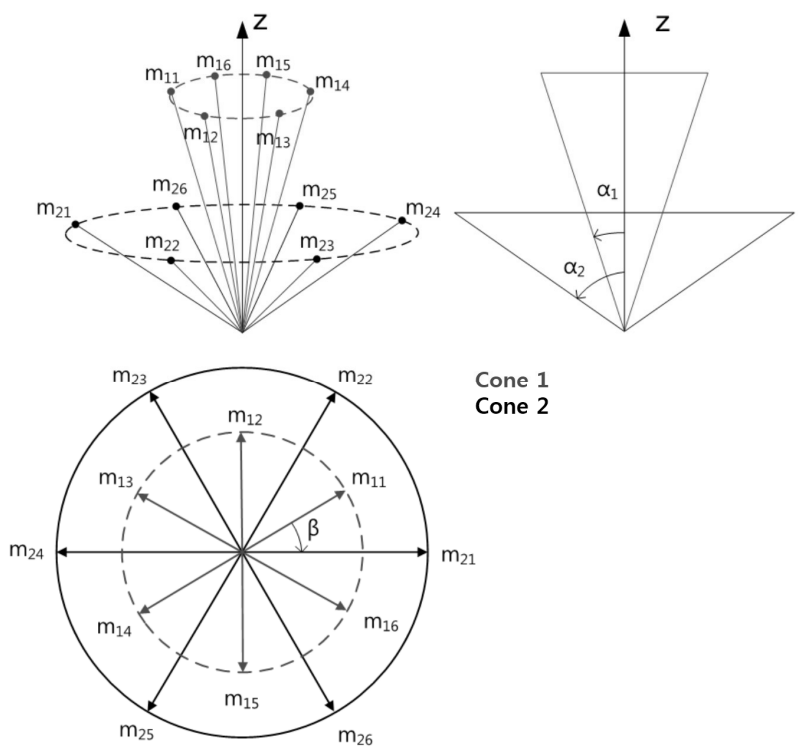

Figure 4.4 Dual conic configuration

In this thesis, optimal solutions of the dual conic configurations are suggested in point of the FDI performance by an analytic approach with the modified form of the FDI performance index in chapter 3. Before the analysis, basic constraint of optimal navigation performance for multiple conic configuration is defined by theorem 1.

Theorem 1: Navigation performance index of RIMU with multiple conic configuration is optimized when geometry of sensors on RIMU satisfies following constraint:

$$\sum_{i=1}^{q} \cos^2 \alpha_i = \frac{q}{3} \tag{4.14}$$

where q is the number of overlapped cones and α_i is a center angle of i^{th} cone as shown in figure 4.4.

Proof: From equation (4.1) and (4.2), DCM of multiple cone is defined as follows:

$$\mathbf{H} = \begin{pmatrix} \tilde{\mathbf{H}}_1^T & \tilde{\mathbf{H}}_2^T & \cdots & \tilde{\mathbf{H}}_q^T \end{pmatrix}^T \tag{4.15}$$

$$\tilde{\mathbf{H}}_i = \begin{pmatrix} \mathbf{h}_{i,1}^T & \mathbf{h}_{i,2}^T & \cdots & \mathbf{h}_{i,n/q}^T \end{pmatrix}^T \tag{4.16}$$

$$\mathbf{h}_{i,k} = \begin{pmatrix} \cos\tilde{\theta}_{i,k} \sin\alpha_i & \sin\tilde{\theta}_{i,k} \sin\alpha_i & \cos\alpha_i \end{pmatrix} \tag{4.17}$$

where n is total number of sensors on RIMU and $\tilde{\mathbf{H}}_i$ is a DCM for i^{th} single cone

following the definition in section 4.2. Since each cone has evenly distributed sensors, $\mathrm{k}=1,2,\cdots,\mathrm{n}/\mathrm{q}$ and the included angle $\tilde{\theta}_{\mathrm{i,k}}$ on i[th] cone as shown in figure 4.4 is defined as follows:

$$\tilde{\theta}_{\mathrm{i,k}}=\frac{2\pi\left(\mathrm{k}-1\right)}{\mathrm{n}/\mathrm{q}}+\beta_{\mathrm{i}} \tag{4.18}$$

where β_i is a twisted angle between standard and i[th] cone along the z-axis. Then, the constraint in (2.19) for optimal navigation performance can be rewritten as follows:

$$\mathbf{H}^{\mathrm{T}}\mathbf{H}=\sum_{\mathrm{i}=1}^{\mathrm{q}}\sum_{\mathrm{j}=1}^{\mathrm{n}/\mathrm{q}}\mathbf{h}_{\mathrm{i,j}}^{\mathrm{T}}\mathbf{h}_{\mathrm{i,j}}=\frac{\mathrm{n}}{3}\mathbf{I}_3 \tag{4.18}$$

$$\sum_{\mathrm{j}=1}^{\mathrm{n}/\mathrm{q}}\mathbf{h}_{\mathrm{i,j}}^{\mathrm{T}}\mathbf{h}_{\mathrm{i,j}}=\begin{pmatrix}\frac{\mathrm{n}}{2\mathrm{q}}\sin^2\alpha_{\mathrm{i}} & 0 & 0\\ 0 & \frac{\mathrm{n}}{2\mathrm{q}}\sin^2\alpha_{\mathrm{i}} & 0\\ 0 & 0 & \frac{\mathrm{n}}{\mathrm{q}}\cos^2\alpha_{\mathrm{i}}\end{pmatrix} \tag{4.19}$$

Therefore, equation (4.18) can be rewritten as follows:

$$\sum_{\mathrm{i}=1}^{\mathrm{q}}\frac{\mathrm{n}}{\mathrm{q}}\cos^2\alpha_{\mathrm{i}}=\frac{\mathrm{n}}{3} \tag{4.20}$$

Finally, the form of the optimal navigation constraint is given as follows:

$$\sum_{i=1}^{q} \cos^2 \alpha_i = \frac{q}{3} \tag{4.21}$$

This is the end of proof.

For case of $q = 2$, there are infinite configurations satisfying the constraint for optimal GNC performance, $\cos^2 \alpha_1 + \cos^2 \alpha_2 = 2/3$. Therefore, it is available to optimize the FDI performance index of dual conic configuration with geometric parameter α_1, α_2 and β as the first cone is set to standard one as shown in figure 4.4. Since α_2 is dependent on α_1, design parameter is reduced to α_1 and β. To avoid repetition of same configurations, the domain of these variables are limited as follows:

$$\alpha_1 < \alpha_2, \quad \cos^{-1}\sqrt{2/3} \le \alpha_1 \le \cos^{-1}\sqrt{1/3}, \quad 0 \le \beta \le 2\pi/n \tag{4.22}$$

and $n \ge 6$ as Gilmore [20] presented. As shown in chapter 3, it is possible to optimize the FDI performance index by minimizing $\varsigma(\varphi_{ij}) = \max_{i,j} |\cos \varphi_{ij}| (j \ne i)$ under the constraint for optimal GNC performance. For dual conic configuration, $\varsigma(\varphi_{ij})$ is determined by one of the following three cases:

Case 1: φ_{ij} is an angle between adjacent two sensors on the first cone.

Case 2: φ_{ij} is an angle between the most widen two sensors on the second cone.

Case 3: φ_{ij} is an angle between adjacent two sensors on different cones.

Therefore, defining ς_k for case 'k', $\varsigma(\varphi_{ij})$ is given as follows:

$$\varsigma(\varphi_{ij}) = \max_{i,j} |\cos\varphi_{ij}| (j \neq i) \;=\; \max[|\varsigma_1|, |\varsigma_2|, |\varsigma_3|] \tag{4.23}$$

$$\varsigma_1 = \left(\cos\frac{2\pi}{n/2} - 1\right)\sin^2\alpha_1 + 1 \tag{4.24}$$

$$\varsigma_2 = \left(\cos\left\{\frac{2\pi}{n/2}\left\lfloor\frac{n}{4}\right\rfloor\right\} - 1\right)\left(\frac{4}{3} - \sin^2\alpha_1\right) + 1 \tag{4.25}$$

$$\varsigma_3 = \cos\beta\sin\alpha_1\sqrt{\frac{4}{3} - \sin^2\alpha_1} + \cos\alpha_1\sqrt{\frac{2}{3} - \cos^2\alpha_1} \tag{4.26}$$

where $\lfloor x \rfloor$ is a floor function, returning the largest integer smaller than x. As differentiating each ς_k by α_1, following inequalities can be obtained as follows:

$$\frac{d\varsigma_1}{d\alpha_1} = 2\left(\cos\frac{2\pi}{n/2} - 1\right)\sin\alpha_1\cos\alpha_1 < 0 \tag{4.27}$$

$$\frac{d\varsigma_2}{d\alpha_1} = 2\left(1 - \cos\left\{\frac{2\pi}{n/2}\left\lfloor\frac{n}{4}\right\rfloor\right\}\right)\sin\alpha_1\cos\alpha_1 > 0 \tag{4.28}$$

$$\frac{d\varsigma_3}{d\alpha_1} = \frac{\cos\beta\cos\alpha_1}{\sqrt{\frac{4}{3} - \sin^2\alpha_1}}\left[\frac{4}{3} - 2\sin^2\alpha_1\right] + \frac{\sin\alpha_1}{3\sqrt{\frac{2}{3} - \sin^2\alpha_1}} \geq 0 \tag{4.29}$$

It means that ς_1 is the monotone decreasing and ς_2, ς_3 are the monotone increasing functions in the domain (4.22). In addition, $\varsigma_1 \geq 0$, $\varsigma_2 \leq 0$, $\varsigma_3 > 0$ at $\alpha_1 = \cos^{-1}\sqrt{1/3}$ and $\varsigma_3 > 0$ at $\alpha_1 = \cos^{-1}\sqrt{2/3}$. Therefore, these inequalities are extended to the whole domain of α_1 and $\varsigma\left(\varphi_{ij}\right)$ is redefined as follows:

$$\varsigma\left(\varphi_{ij}\right) = \max[\varsigma_1, -\varsigma_2, \varsigma_3] \tag{4.30}$$

Meanwhile, the FDI performance index is inversely proportional to $\varsigma\left(\varphi_{ij}\right)$ and the optimal configuration that maximize the FDI performance index is set on the lowest point of $\varsigma\left(\varphi_{ij}\right)$. This point is defined as "optimal point" for dual conic configuration as shown in figure 4.5. The lower the optimal point is, the higher the FDI performance index is from the definition of $\varsigma\left(\varphi_{ij}\right)$. Additionally, ς_3 moves to α_1-axis in figure 4.5 as $\cos\beta$ is minimized. It means that the optimal point lower as $\cos\beta$ is minimized since each ς_k follows the inequalities (4.27) ~ (4.29). Therefore, β has to be $2\pi/n$ to minimize $\cos\beta$. Also, $\varsigma_1, -\varsigma_2 \leq \varsigma_3$ at the upper bound $\alpha_1 = \cos^{-1}\sqrt{1/3}$ and $\varsigma_1, -\varsigma_2 \geq \varsigma_3$ at the lower bound $\alpha_1 = \cos^{-1}\sqrt{2/3}$. Since all ς_k is continuous in the domain, there exist intersections $\left(s, \varsigma_3(s)\right)$ where $s \in X$ and

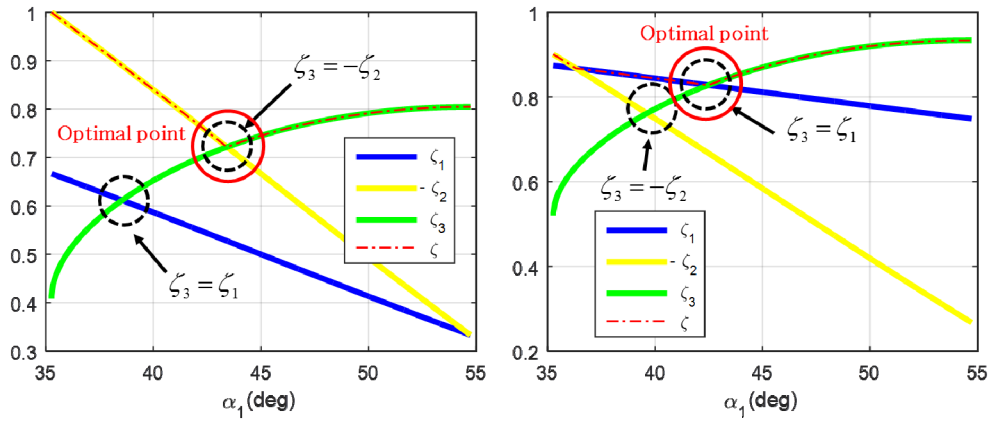

(a) The number of sensors : 8 (b) The number of sensors : 14

Figure 4.5 Optimal point on $\varsigma(\varphi_{ij})$ and ς_k

X is defined as follows:

$$X := \{\alpha_1 | \varsigma_3(\alpha_1) = \varsigma_1(\alpha_1),\ \varsigma_3(\alpha_1) = -\varsigma_2(\alpha_1)\} \tag{4.31}$$

It is obvious that one of the intersections is the optimal point as shown in figure 4.5. Then, the optimal solution for the FDI performance index of dual conic configuration is determined as follows:

$$\beta = \frac{2\pi}{n},\ \xi = \max(\varsigma_3(s)),\ \alpha_1 = \varsigma_3^{-1}(\xi) \tag{4.32}$$

4.4 Performance Index Comparison

To evaluate the optimization approach based on the modified form of the FDI performance index, the analytic solutions of optimal dual conic configurations are compared with the numerically calculated values. To find the numerical results, the FDI performance index is calculated for all dual conic configuration with 0.01° resolution. As shown in table 4.3, the analytic solutions are identical to the numerical ones.

Table 4.3 Geometry for optimal FDI performance of dual conic configuration

n	α_1 (deg)		β (deg)	
	Analytic	Numerical	Analytic	Numerical
6	37.37	37.37	60	60
8	43.42	43.42	45	45
10	39.97	39.97	36	36
12	41.54	41.54	30	30
14	42.48	42.47	25.71	25.71
16	43.48	43.48	22.5	22.5
18	44.36	44.35	20	20
20	45.1	45.1	18	18

The FDI performance indices of the optimized dual conic configurations in table 4.3 are compared with the ones of the platonic solids and single conic configuration introduced in aforementioned section. Since there is no room to optimize the FDI performance index of platonic solids and single conic configurations, their optimal solutions are set by their constraint of optimal GNC performance. On table 4.4, the higher the index is, the better FDI performance is and it is clear that the optimized dual conic configurations achieves better FDI performance.

Table 4.4 Comparison result of the FDI performance index

n	FDI performance index		
	Platonic solids (type 1~6)	Single conic configuration	Optimized dual conic configuration
6	1	2.250	4.999
8	2.778	4.298	5.331
10	-	7.149	10.656
12	9	10.852	14.525
14	-	15.412	19.595
16	-	20.839	25.313
18	-	27.138	31.872
20	32.105	34.314	39.280

4.5 Summary

In this chapter, the FDI performance of platonic solid, single conic and dual conic configurations is optimized under the constraint of the optimal GNC performance confirmed in chapter 2. For the optimization, the modified form of the FDI performance index newly suggested in chapter 3 is applied. As a result, it is confirmed that the analytic solution of the configurations for the optimal FDI performance index is identical to that of numerical approach which means that the newly suggested, modified form of the FDI performance index is reasonable for the FDI performance optimization. Moreover, it is confirmed that FDI performance index of dual conic configuration optimized by the analytic approach using the new form of the FDI performance index is superior to the ones of the platonic solid and single conic configuration.

Chapter 5

Simulation and Experiment

5.1 Numerical Simulation

In chapter 4, it is confirmed that the FDI performance of the optimized dual conic configuration is better than that of others such as platonic solids and single conic configurations by using the FDI performance index. However, this is an indirect approach and it is unknown how the RIMU system would response to the fault in real conditions. Therefore, the FDI performance of RIMU needs to be certified by simulations under the assumption of the fault on sensors. The FDI performance of RIMU can be defined by false alarm, miss detection and correct isolation rate [2]. In this chapter, Probability of Correct Isolation (PCI) is applied to confirmed how well the PSA-based FDI algorithm can identify the fault position when the bias fault is added to one of the sensor measurements on each RIMU configuration. The fault size is expressed in a Fault to Noise Ratio (FNR) and PCI values are determined by 1000 times Monte Carlo simulations. In the simulations, threshold is set to 3 times of the standard deviation of sensor noise. Simulation results are shown in figure 4.6 ~ 4.9.

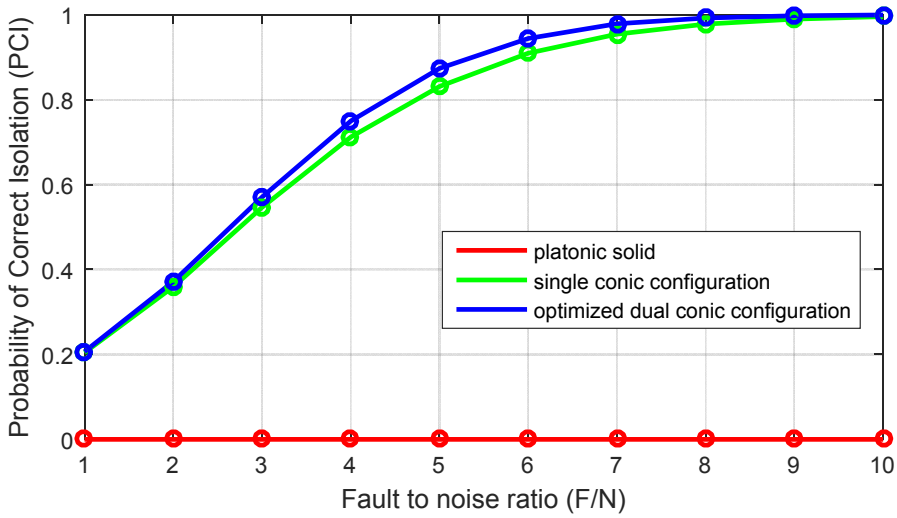

Figure 5.1 F/N – PCI graph for n=6

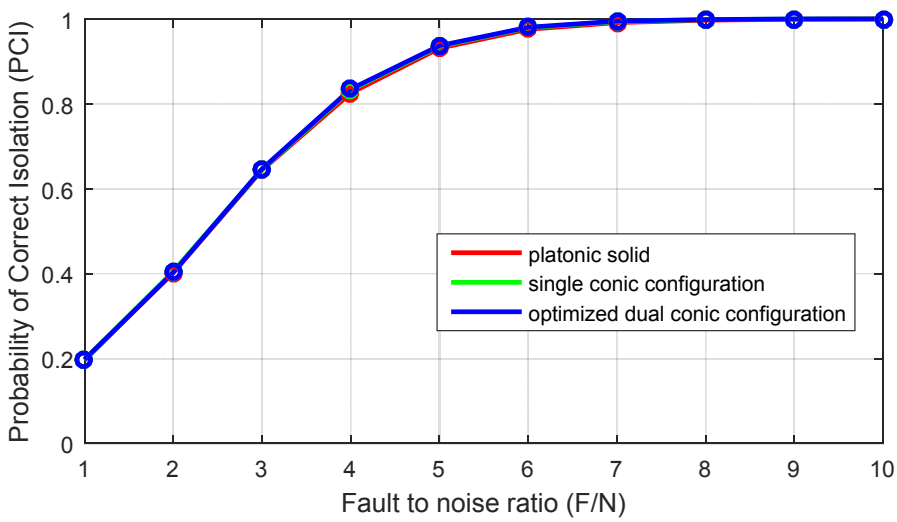

Figure 5.2 F/N – PCI graph for n=8

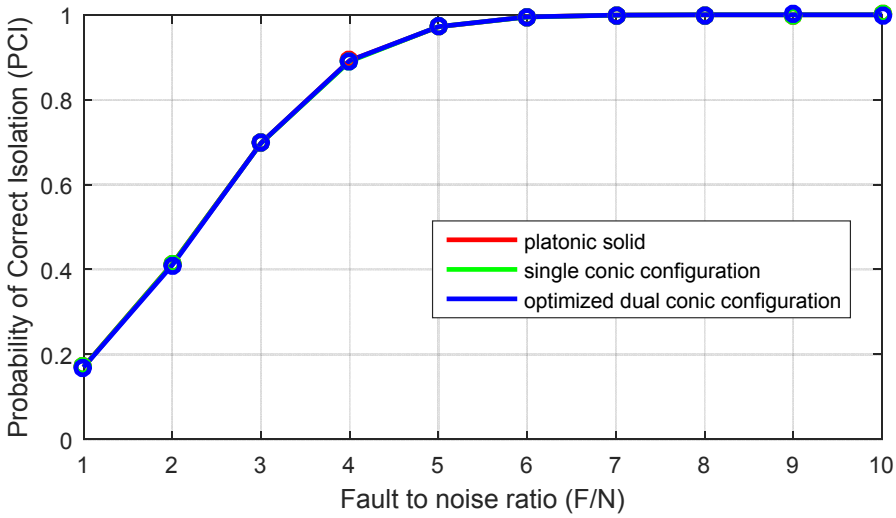

Figure 5.3 F/N – PCI graph for n=12

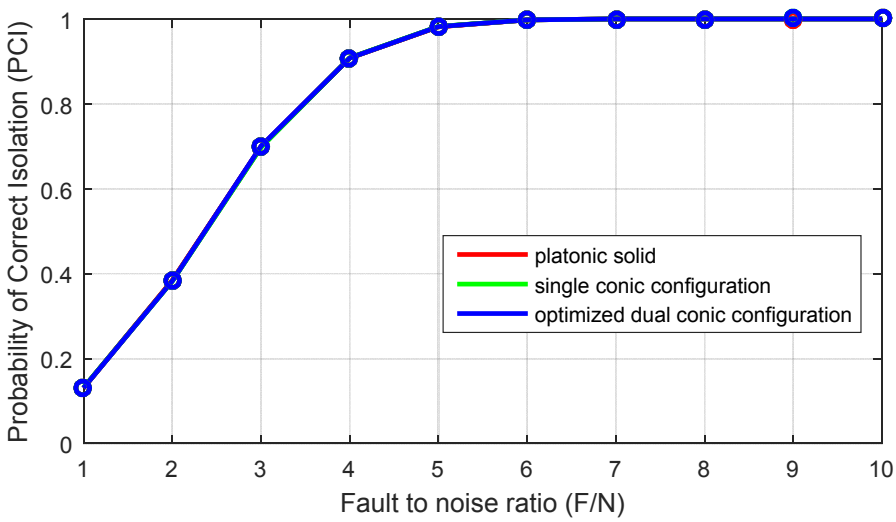

Figure 5.4 F/N – PCI graph for n=20

In figure 5.1, PCI value of each configuration tends to be identical to the comparison results using FDI performance index. Using 6 sensors on RIMU, it is expected that the platonic solid configuration, also can be called the cubic configuration for $n=6$, cannot identify which sensor is on fault since its FDI performance index is one in table 4.4 and the same result is confirmed by the simulation result in figure 5.1. Also, in figure 5.1, it is shown that the PCI of the optimized dual conic configuration is superior to the one of the single conic configuration as expected by the FDI performance index in table 4.4. When using more than 8 sensors, however, it is confirmed that there is little distinction between the PCI of the configurations with different FDI performance index as shown in figure 5.2 ~ 5.4. It means that there is no particular difference in the FDI performance of platonic solids, single conic and dual conic configurations regardless of the FDI performance index of each configuration. The reason of this result is expected in the definition of the FDI performance index. From the definition in chapter 2.3, the FDI performance index is determined by the parity ratio of the fault axis and non-fault axis while the terms related to the sensor noises are canceled out each other. Meanwhile, it is confirmed that the FDI performance of each configuration becomes similar as the number of the inertial sensors increases. Then, the differences of the parity responses for each configuration are expected to be lower than the noise level as the number of sensors increases and current index for FDI performance loses its meaning.

5.2 Experiment on Sensor Frame

As verified in simulations in chapter 5.1, the FDI performance of each configuration has no meaningful difference as the number of sensors increases more than eight even though the FDI performance indices are different. If the RIMU uses six sensors, however, each configuration has different FDI performance in simulation as expected by the comparison of the index. Therefore, FDI experiments using 3D-printed frame and analog gyros are conducted to verify the above results for the case of $n=6$. The fault is assumed as a bias on a randomly selected sensor and the parity responses for this fault are measured. For the experiments, ENC03-RC-R analog gyros of Murata Manufacturing Co., Ltd. are applied with analog signal amplifier and filter circuits as shown in figure 5.5. The design model of the frames are shown in figure 5.6 and 5.7 while their 3D-printed output with the gyro modules are shown in figure 5.8 and 5.9.

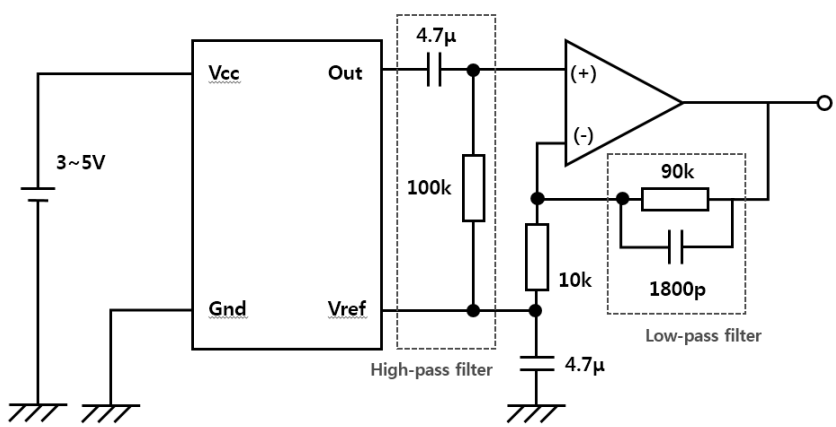

Figure 5.5 Schematic of ENC03-RC analog gyro and amplifier/filter circuit

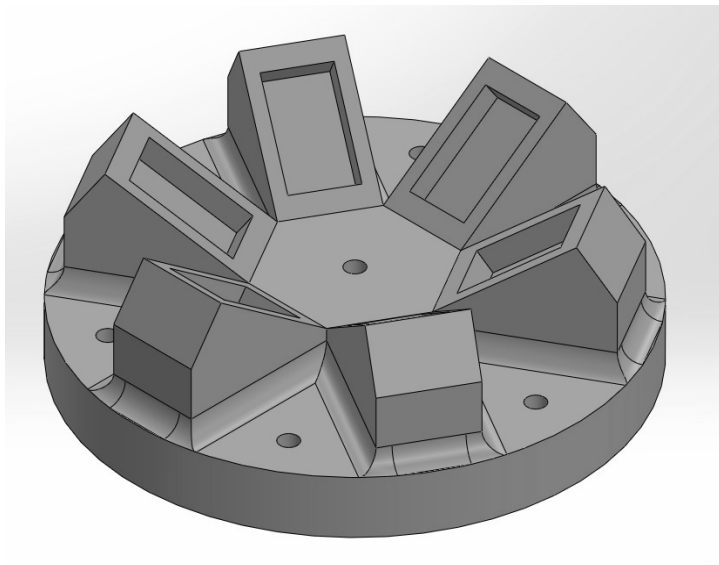

Figure 5.6 3D-CAD model of sensor frame for single conic configuration

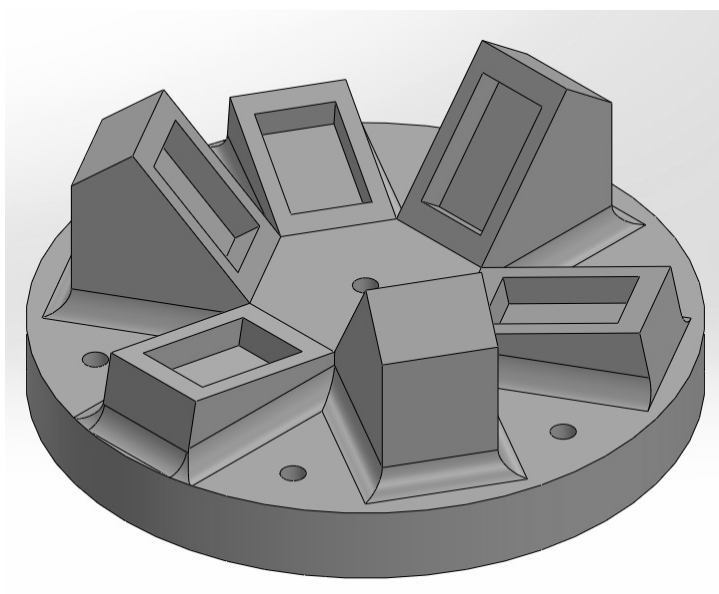

Figure 5.7 3D-CAD model of sensor frame for dual conic configuration

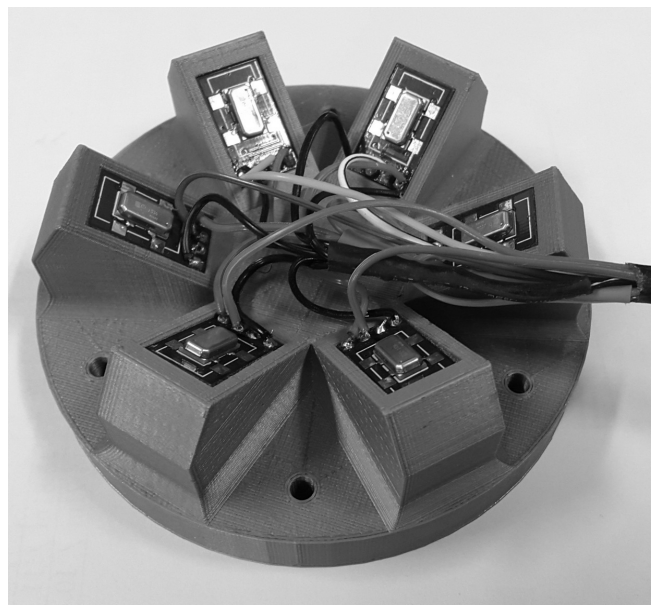

Figure 5.8 Frame for single conic configuration

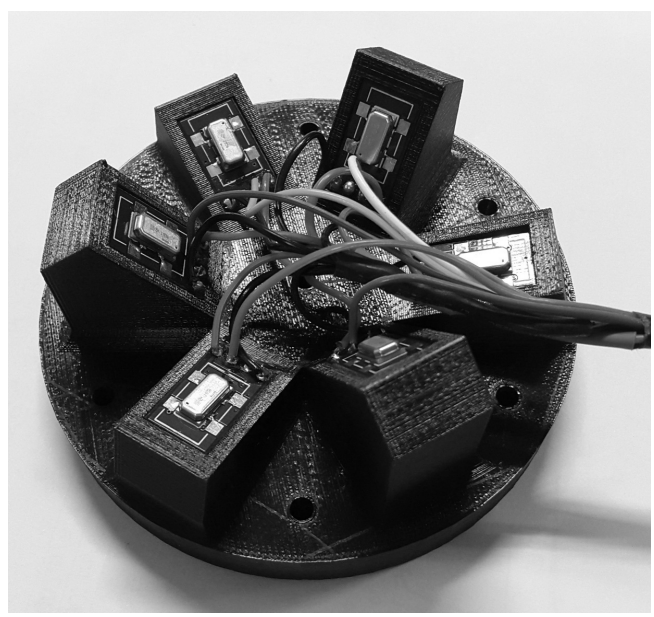

Figure 5.9 Frame for dual conic configuration

Table 5.1 Experiment condition

Condition	value
The number of sensors	6
Standard deviation of sensor noise (σ)	0.3938deg/sec
Sampling rate	100Hz
System dynamics	Random
Threshold (T)	3σ
Fault type	Bias
Fault to Noise Ratio (FNR)	0 to 10

Conditions for the experiments are shown in table 5.1. The standard deviation of sensor noise is calculated by measurements in steady state since the manufacturer does not provide related information. The experiments are conducted as shown in figure 5.10. Increasing the FNR of bias fault on a randomly selected sensor, parity responses for each sensor input axis are monitored. Figure 5.11 shows the parity responses when the bias fault whose size is FNR=4 is occurred on the sensor monitored by $\mathbf{p}_{\text{fault}}$ while $\mathbf{p}_{\text{k}}$ is selected as the parity that responds most similarly to $\mathbf{p}_{\text{fault}}$. It is clear that it is more easy to distinguish $\mathbf{p}_{\text{fault}}$ and $\mathbf{p}_{\text{k}}$ on the optimized dual conic configuration as predicted by the comparison of FDI performance index and PCI simulations. The same results are also shown in table 5.2 as the difference between $\mathbf{p}_{\text{fault}}$ and $\mathbf{p}_{\text{k}}$ is larger on

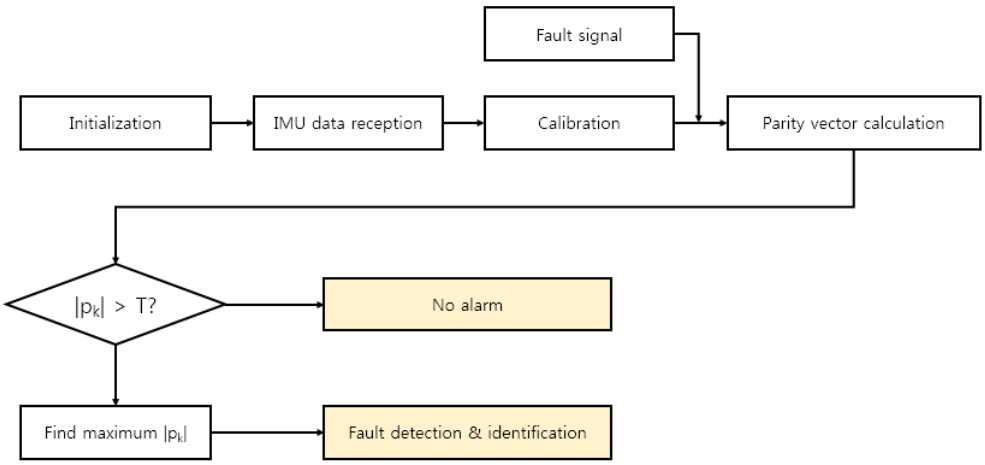

Figure 5.10 Sequence of FDI experiment on sensor frames

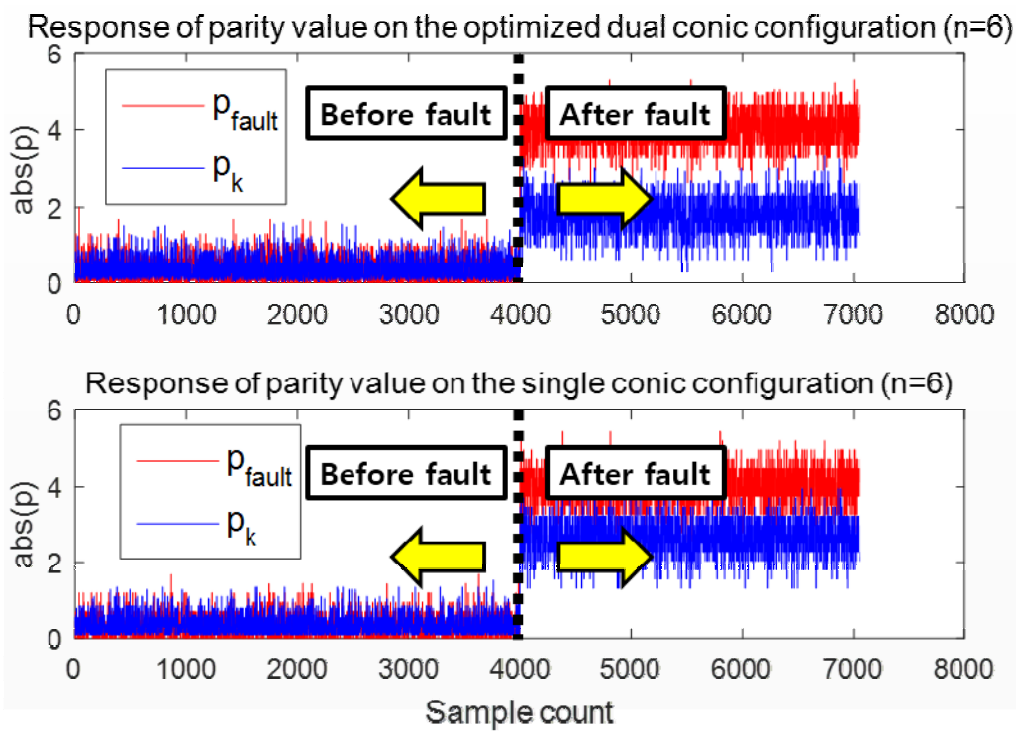

Figure 5.11 Experimental result of parity responses (FNR = 4)

Table 5.2 Parity response ratio with respect to FNR

FNR	Single cone / Dual cone		
	$E(\mathbf{p}_{fault})$	$E(\mathbf{p}_k)$	$E(\mathbf{p}_{fault}) - E(\mathbf{p}_k)$
1	1.0392 / 1.0923	0.7028 / 0.4654	0.3364 / 0.6269
2	2.0395 / 2.0617	1.3695 / 0.9128	0.6700 / 1.1489
3	3.0070 / 3.0581	2.0395 / 1.3602	0.9709 / 1.6979
4	4.0334 / 4.0205	2.6623 / 1.8076	1.3711 / 2.2129
5	5.0952 / 5.0837	3.3695 / 2.2550	1.7257 / 2.8287
6	6.0035 / 6.0729	4.0361 / 2.7024	1.9674 / 3.3705
7	7.0182 / 7.0141	4.7028 / 3.1498	2.3154 / 3.8643
8	8.0728 / 8.0643	5.3695 / 3.5972	2.7033 / 4.4671
9	9.0085 / 9.0816	6.0361 / 4.0446	2.9724 / 5.0370
10	10.0598/ 10.0422	6.7028 / 4.4844	3.3570 / 5.5578

the optimized dual conic configuration. Therefore, FDI performance of the RIMU using 6 sensors can be improved by applying the newly suggested, optimal dual conic configurations.

Chapter 6

Conclusions

The RIMU is an effective system to improve the reliability of the inertial navigation system and there exists optimal configuration of RIMU since the performance of RIMU is dependent on its configuration. In this thesis, the optimal solutions of the RIMU configurations with respect to the FDI performance and the GNC performance are suggested by geometric analysis approach. For the analysis, the modified FDI performance index is newly suggested as a function of geometric parameter of the angle between sensors. Since this index consider the constraint for the optimal GNC performance of RIMU, it is possible to optimize the FDI performance of the configurations while the optimal GNC performance is achieved. By using this new index, optimal solutions of platonic solids, single conic and dual conic configurations are confirmed. As a result, it is confirmed that the optimized dual conic configuration has the FDI performance index superior to that of other configurations. To verify this result, Monte Carlo simulations to calculate the PCI of each configuration under the sensor bias fault condition are conducted. The same result of the performance index comparison is also confirmed by the simulation for the RIMU utilizes six sensors. As the number of sensors increases more than 8, however, it is confirmed that there is no particular difference in the FDI performance of each configuration regardless of the FDI performance index. The reason is expected that the differences of the parity responses for each configuration lower than the noise level. Therefore, FDI

performance index including sensor noise is required for the future works. Meanwhile, the experiments using six sensors on 3D-print frames are conducted. As a result, it is confirmed that the FDI performance of the RIMU using six sensors can be improved by applying the newly suggested, optimal dual conic configuration.

Bibliography

[1] M. E. Pittelkau, "Cascaded and Decoupled RIMU Calibration Filters," *J. Astronaut. Sci.*, Vol. 54, No. 3, pp.449-466, 2006.

[2] D. S. Shim and C. K. Yang, "Optimal Configuration of Redundant Inertial Sensors for Navigation and FDI performance," *Sensors*, Vol. 10, pp. 6497-6512, 2010.

[3] J. O. Nilsson, I. Skog and P. Händel, "Aligning the Forces – Eliminating the Misalignments in IMU Arrays," *IEEE Trans. Inst. Meas.*, Vol. 63, No. 10, pp. 2498-2500, 2014.

[4] S. Sukkarieh, P. Gibbens, B. Grocholsky, K. Willis and H. F. Durrant-whyte, "A Low-Cost, Redundant Inertial Measurement Unit for Unmanned Air Vehicles," *Int. J. Robot. Res.*, Vol. 19, No. 11, pp. 1089-1103, 2000.

[5] S. Yoon, S. Kim, J. Bae, Y. Kim and E. Kim, "Experimental evaluation of fault diagnosis in a skew-configured UAV sensor system," *Control Eng. Pract.*, Vol. 19, No. 2, pp. 153-173, 2011.

[6] K. H. Kim, D. S. Shim, C. G. Park and J. G. Lee, "Optimal IMU Configuration for a SDINS," *in Proc. ICCAS 2001*, Jeju, Republic of Korea, 2001.

[7] I. Hwang, S. Kim, Y. Kim and C. E. Seah, "A Survey of Fault Detection, Isolation, and Reconfiguration Methods," *IEEE Trans. Control Syst. Tech.*, Vol. 18, No. 3, pp. 636-653, 2010.

[8] W. Lee and C. G. Park, "A Fault Detection Method of Redundant IMU Using Modified Principal Component Analysis," *Int. J. Aeronaut. Space Sci.*, Vol. 13, 398-404, 2012.

[9] W. Lee and C. G. Park, "Double Fault Detection of Cone-Shaped Redundant IMUs Using Wavelet Transformation and EPSA," *Sensors*, Vol. 14, 3428-3444, 2014.

[10] R. Weiss and I. Nathan, "An Ultrareliable Sensing System for Vehicles with Limited Sparing Capability," *J. Spacecraft*, Vol. 4, No. 9, pp.1151-1158, 1967.

[11] L. Gomes, G. Yuksel, V. Lappas, A. S. Curiel, A. Bradford, C. Ozkaptan and M. Sweeting, "BILSAT: Advancing Smallsat Capabilities," *in Proc. AIAA/USU Conference on Small Satellites 2003*, Logan, UT, USA, 2003.

[12] D. E. Bittner, J. A. Christian, R. H. Bishop and D. May, "Fault Detection, Isolation, and Recovery Techniques for Large Clusters of Inertial Measurement Units," *in Proc.* IEEE/ION *PLANS 2014*, Monterey, CA, USA, 2014.

[13] A. Waegli, S. Guerrier and J. Skaloud, "Redundant MEMS-IMU integrated with GPS for performance assessment in sports," *in Proc.* IEEE/ION *PLANS 2008*, Monterey, CA, USA, 2008

[14] I. Skog, J. O. Nilsson, P. Händel and Arye Nehorai, "Inertial Sensor Arrays, Maximum Likelihood, and Cramer-Rao Bound," *arXiv preprint arXiv:1509.06494v2, 2016.*

[15] J. C. Wilcox, "Competitive Evaluation of Failure Detection Algorithms for Strapdown Redundant Inertial Instruments," *J. Spacecraft*, Vol. 11, No. 7, pp. 525-530, 1974.

[16] J. V. Harrison and G. Gai, "Evaluating Sensor Orientations for Navigation Performance and Failure Detection," *IEEE Trans. Aerosp. Electron. Syst*, Vol. AES-13, No. 6, pp. 631-643, 1977.

[17] J. Y. Kim, C. K. Yang and D. S. Shim, "Navigation and Fault Detection Performance Analysis for INS Redundant Sensor Configurations," *J. Control, Autom. Syst. Eng.*, Vol. 8, No. 8, pp. 698-705, 2002.

[18] H. Jin and H. Y. Zhang, "Optimal Parity Vector Sensitive to Designated Sensor Fault," *IEEE Trans. Aerosp. Electron. Syst*, Vol. 35, No. 4, pp. 1122-1128, 1999.

[19] M. K. Jeerage, "Reliability Analysis of Fault-Tolerant IMU Architectures with Redundant Inertial Sensors," *in IEEE/ION Proc. PLANS '90*, Las Vegas, NV, USA, 1990.

[20] J. P. Gilmore and R. A. Mckern, "A Redundant Strapdown Inertial Reference Unit (SIRU), *J. Spacecraft*, Vol. 9, No. 1, pp. 39-47, 1972.

국문초록

본 논문에서는 기하학적 파라미터의 분석을 통해 고장검출 및 판별 성능 측면에서 중첩관성센서의 최적의 배치 형상을 제시하였다. 각 배치형상에 대한 고장검출 및 판별 성능을 정의하기 위하여, 패리티 공간 기법에 기반한 성능지표를 사용하였다. 하지만 해당 지표는 배치형상의 방향코사인 행렬에 대한 영공간에 대한 함수이기 때문에, 직접적인 분석이 어렵다는 단점이 있었다. 또한 최적항법성능을 위한 조건을 고려하지 못한다는 한계도 있었다. 이를 해결하기 위해, 센서의 배치형상에 대한 기하학적 파라미터로 표현되는 수정된 형태의 고장검출 및 판별 성능지표를 새롭게 제안하였으며, 원활한 분석 및 최적화 기반을 확보하였다. 이를 통해 정다면체, 단일 원추 배치와 같은 기존 형상과 함께 이중 원추 배치 형상에 대한 고장검출 및 판별 성능지표에 대한 최적화를 수행하여 값을 비교하였다. 그 결과, 최적화된 이중 원추 배치 형상을 사용하면 다른 배치 형상을 사용할 때보다 같은 개수의 중첩 센서에 대한 고장검출 성능지표가 향상되는 것을 확인하였다. 또한 이에 대한 실험 및 시뮬레이션을 통해 성능지표를 사용한 비교 결과의 타당성에 대해 검증하였다.

주요어: 고장검출 및 판별, 중첩관성센서, 패리티 공간 기법, 성능지표, 센서배치형상, 최적화

이 름: 김 현 진

학 번: 2013-20666